

The same expression, with  $L_T$  replaced by  $l_H = \sqrt{\pi\hbar c/eH}$ , determines  $\mathcal{J}(0, H)$  in the presence of a weak transverse magnetic field  $H$ . To find the critical temperature  $T_c(b)$  and the  $T = 0$  value of the upper critical field  $H_{c2}$ , one uses Eqn (2) together with Eqns (22), (25). The result is that both  $T_c(g)$  and  $H_{c2}(g)$  scale in the same way, and drop fast at  $b \rightarrow b_c(g)$ :

$$\ln \frac{T^*}{T_c} \approx \ln \frac{\Phi_0}{H_{c2} b^2} \approx \frac{2 \ln(b/d)}{b_c^2(g)/b^2 - 1}, \quad (26)$$

where  $T^* = \hbar D/b^2$ , and  $\Phi_0 = hc/2e$  is the flux quantum. The form of Eqn (26) suggests that the behavior of the array near the quantum critical point  $b = b_c(g)$  can be understood in terms of the standard BCS-type theory with a macroscopic effective Cooper attraction  $\lambda_{\text{eff}}$ , which vanishes at  $b \rightarrow b_c(g)$ . Equation (26) is valid for  $b/b_c(g) \geq [2 \ln(b/d)]^{-1/2}$ . This inequality ensures that  $T_c$  is small compared both to  $T^*$  (under this condition the proximity coupling is long-range) and to  $\hbar/C(0)$ . The latter condition allows one to approximate  $\mathcal{C}(T)$  by  $\mathcal{C}(0)$  while deriving Eqn (26). At shorter  $b \ll b_c(g) \sqrt{\lambda_g}$ , the transition occurs at  $T_c \sim T^*$ . Here  $L_{T_c} \sim b$ , the MFA is not applicable and the transition is governed by thermal fluctuations. Similarly, the characteristic scale of magnetic field which affects superconductive state in such an array is just  $\Phi_0/b^2$ : at higher fields formation of a superconductive glass state is expected. Additional limitation for our results from the higher- $T$  side is due to the neglect of quasi-particles inside SC islands, the corresponding temperature scale being  $T_{\text{parity}} = \Delta_{\text{SC}}/\ln(vV_i \Delta_{\text{SC}})$ . On the other hand, the conclusion about metallic nature of the system's state at  $b > b_c(g)$  is limited to the temperature scale  $T \geq T_{\text{loc}} \sim \hbar \omega_d \exp(-\pi^2 g)$ , since we neglected weak localization effects (the value of  $g$  entering this estimate is defined at the length scale of the order of  $d$ ). Determination of weak-localization corrections to the conductance of an array with  $b > b_c(g)$  would need the account of dephasing effects due to fluctuations of island's phases. This is an interesting problem which we left for the future studies.

Finally, we comment briefly on the similar problem of small superconductive grains of radius  $d$  immersed into a 3D metal with bulk resistivity  $\rho$ . In this case the simple method of Ref. [18] can be used. The characteristic Coulomb energy  $\hbar/C(0) \approx \hbar \omega_d \exp(-\pi\hbar/4e^2 R_A)$  in the tunneling limit  $R_T \gg R_N$ ; here  $R_A = R_T^2/R_N$  and  $R_N = \rho/4\pi d$ . Proximity coupling energy is estimated as  $J(r) \sim (\hbar/e^2 R_T)^2/r^3 v$ . The point of the SC-M transition is then given by  $\hbar\rho/16e^2 d R_T^2 \cong 3 \ln b/d$ .

In conclusion, we developed a theory of quantum superconductive-metal transition in a 2D proximity-coupled array. The critical resistance  $R_{\square c}$  is non-universal and small compared to the quantum resistance. Near the quantum critical point the system behaves as a BCS-like superconductor with the effective Cooper attraction constant vanishing at  $R_{\square} \rightarrow R_{\square c}$ .

We are grateful to A Kamenev and Yu V Nazarov for useful discussions. This research was supported by the NSF grant DMR-9812340 (A I L), RFBR grant 98-02-16252, NWO–Russia collaboration grant, Swiss NSF–Russia collaboration grant 7SUPJ062253.00 and by the Russian Ministry of Industry, Science and Technology via the project ‘‘Mesoscopic electron systems for quantum computing’’ (M V F and M A S).

## References

1. Fisher M P A *Phys. Rev. Lett.* **65** 923 (1990)
2. Goldman A M, Markovic N *Phys. Today* **51** (11) 39 (1998)
3. van der Zant H S J et al. *Phys. Rev. Lett.* **69** 2971 (1992); *Phys. Rev. B* **54** 10081 (1996)
4. Gantmakher V F et al. *Pis'ma Zh. Eksp. Teor. Fiz.* **71** 231 (2000) [*JETP Lett.* **71** 160 (2000)]
5. Chervenak J A, Valles J M, Jr. *Phys. Rev. B* **61** R9245 (2000)
6. Mason N, Kapitulnik A, cond-mat/0006138
7. Efetov K B *Zh. Eksp. Teor. Fiz.* **78** 2017 (1980) [*Sov. Phys. JETP* **51** 1015 (1980)]
8. Fazio R, Schön G *Phys. Rev. B* **43** 5307 (1991)
9. Delsing P et al. *Phys. Rev. B* **50** 3959 (1994)
10. Jaeger H M et al. *Phys. Rev. B* **40** 182 (1989)
11. Haviland D B, Liu Y, Goldman A M *Phys. Rev. Lett.* **62** 2180 (1989)
12. Gantmakher V F et al. *Pis'ma Zh. Eksp. Teor. Fiz.* **64** 713 (1996) [*JETP Lett.* **64** 767 (1996)]
13. Hebard A F, Paalanen M A *Phys. Rev. Lett.* **65** 927 (1990)
14. Finkel'stein A M *Pis'ma Zh. Eksp. Teor. Fiz.* **45** 37 (1987) [*JETP Lett.* **45** 46 (1987)]; *Sov. Sci. Reviews Sect. A Phys. Rev.* (Ed. I M Khalatnikov) **14** (Pt. 2) 3 (1990)
15. Finkel'stein A M *Physica B* **197** 636 (1994)
16. Larkin A I *Ann. Phys. (Leipzig)* **8** 507 (1999)
17. Schmid A *Phys. Rev. Lett.* **51** 1506 (1983); Bulgadaev S A *Pis'ma Zh. Eksp. Teor. Fiz.* **39** 264 (1984) [*JETP Lett.* **39** 315 (1984)]
18. Feigel'man M V, Larkin A I *Chem. Phys.* **235** 107 (1998)
19. Spivak B Z, Zyuzin A, Hruska M, cond-mat/0004058
20. Aslamazov L A, Larkin A I, Ovchinnikov Yu N *Zh. Eksp. Teor. Fiz.* **55** 323 (1968) [*Sov. Phys. JETP* **28** 171 (1969)]
21. Vaks V G, Larkin A I, Pikin S A *Zh. Eksp. Teor. Fiz.* **53** 313 (1967) [*Sov. Phys. JETP* **26** 188 (1968)]
22. Usadel K *Phys. Rev. Lett.* **25** 507 (1970); Nazarov Yu V *Phys. Rev. Lett.* **73** 1420 (1994)
23. Feigel'man M V, Larkin A I, Skvortsov M A *Phys. Rev. B* **61** 12361 (2000)
24. Kosterlitz J M *Phys. Rev. Lett.* **37** 1577 (1976)
25. Hekking F W J, Nazarov Yu V *Phys. Rev. B* **49** 6847 (1994)
26. Skvortsov M A, Larkin A I, Feigel'man M V *Phys. Rev. B* **63** 134507 (2001)
27. Zhou F et al. *Phys. Rev. B* **52** 4467 (1995); Stoof T H, Nazarov Yu V *Phys. Rev. B* **53** 14496 (1996)
28. Al'tshuler B L, Aronov A G, Lee P A *Phys. Rev. Lett.* **44** 1288 (1980)
29. Kamenev A, Andreev A F *Phys. Rev. B* **60** 2218 (1999)

## Fluctuation effects in high sheet resistance superconducting films

J M Valles Jr., J A Chervenak, S-Y Hsu, T Kouh

**Abstract.** As the normal-state sheet resistance,  $R_n$ , of a thin-film superconductor increases, its superconducting properties degrade. For  $R_n \simeq h/4e^2$  superconductivity disappears and a transition to a nonsuperconducting state occurs. We present electron tunneling and transport measurements on ultrathin, homogeneously disordered superconducting films in the vicinity of this transition. The data provide strong evidence that fluctuations in the amplitude of the superconducting order parameter dominate the tunneling density of states and the resistive transitions in this regime. We briefly discuss possible sources of these amplitude fluctuation effects. We also describe

J M Valles Jr., J A Chervenak, T Kouh Department of Physics, Brown University, Providence, RI USA

S-Y Hsu Department of Electrophysics, National Chiao Tung University, Hsinchu 300, Taiwan

## how the data suggest a novel picture of the superconductor-to-nonsuperconductor transition in homogeneous 2D systems.

### 1. Introduction

It has been known for some time that increasing the normal-state sheet resistance,  $R_n$ , of a homogeneously disordered (as opposed to islanded) superconducting film reduces its mean-field transition temperature,  $T_{c0}$  and superconducting energy gap  $\Delta$  [1, 2]. For  $R_n$  comparable to  $h/4e^2$ ,  $T_{c0}$  [3] and  $\Delta$  [4] approach zero and a superconductor-to-non-superconductor transition (SNST), commonly referred to as a superconductor-to-insulator transition (SIT), takes place (see Fig. 1). Close to this transition, variations in the density of electronic states on mesoscopic length scales [5], disorder enhanced inelastic scattering processes [2, 6] and proximity to the quantum critical point separating a superconducting from a non-superconducting phase [7, 8] are expected to cause large, non-mean field like fluctuations in the amplitude of the superconducting order parameter. Finding evidence of these effects is interesting because it can provide insight into the nature of the nonsuperconducting phase and the physics driving the SNST.

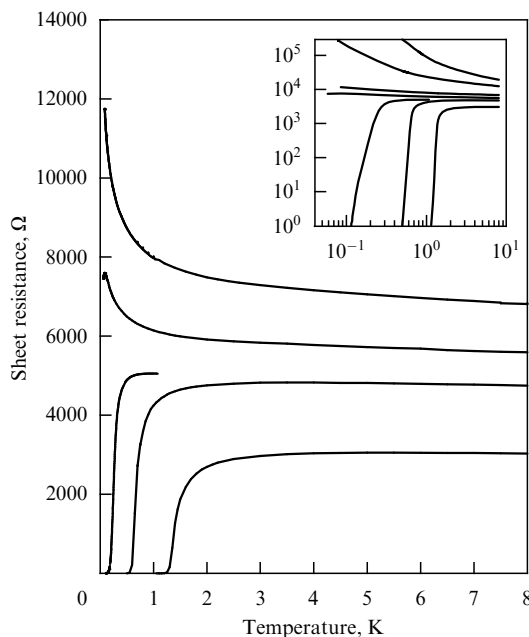


**Figure 1.** Temperature dependence of the sheet resistance of Bi/Sb films of varying thickness. The inset shows that films with sheet resistances at 8 K much greater than 10 k $\Omega$  exhibit ‘insulating-like’ behavior and films with sheet resistances at 8 K much less than 10 k $\Omega$  superconduct with relatively sharp transitions. The main body of the figure shows the data in the transition region between these two extremes. The superconducting transitions move to lower temperature with increasing normal-state sheet resistance,  $R_n = R(8K)$ .

In this paper, we present tunneling and transport data on homogeneous films in this regime that show evidence of large amplitude fluctuations. The tunneling measurements indicate that the fluctuations increase the quasi-particle density relative to the Cooper pair density or equivalently, increase the normal fluid fraction. The transport measurements suggest that the paraconductance or amplitude fluctuation dominated regime of the resistive transitions grows and

diverges in size at the SNST (SNST). Taken together, the experiments intimate that amplitude fluctuation effects drive down the superfluid density, by increasing the quasi-particle density to drive the SNST in homogeneous films and the non-superconductor consists of weakly localized quasi-particles. This scenario contrasts sharply with the prevalent dirty boson models of a SIT, which attribute the reduction in the superfluid density to the reduction of Josephson coupling between spatially separated film regions [9, 10].

### 2. Experimental details

The quench-condensed films that we have studied are homogeneous Bi/Sb and PbBi/Ge. They were deposited on fire-polished glass substrates held near 4 K on the cold stage of a dilution refrigerator [11, 12]. They consist of a two to three monolayer-thick *in situ* deposited amorphous layer of Sb or Ge that does not conduct at low temperatures covered by subsequent evaporations of Bi or PbBi. Experiments [11, 12] indicate that these films have a uniform morphology. First, they become electrically continuous after deposition of as little as 1–2 bulk monolayers worth of the metal as measured by a quartz microbalance. They superconduct at 3–4 bulk monolayers. Second, their conductance as a function of thickness indicates that the elastic mean free path is of the order of an interatomic spacing and changes very little with metal film thickness. Finally, *in situ* scanning tunneling microscopy measurements on a similar system imply that the films have a smooth, rather than a granular or islanded, morphology [13]. The transport and tunneling measurements that we present here were obtained using standard, four-terminal, low-level AC and DC techniques. For a BCS s-wave superconductor, the normalised differential tunnel junction conductance gives a direct measure of the superconducting quasiparticle density of states,  $N_s(E) = E/(E^2 - \Delta^2)^{1/2}$  where  $E$  is measured relative to the Fermi energy and  $\Delta$  is the superconducting energy gap. At finite temperatures, the voltage-dependent conductance qualitatively resembles the density of states. At low temperatures,  $T < 0.5$ , the voltage at which the differential conductance crosses 1 corresponds closely to  $\Delta/e$ .

### 3. Results

Tunneling and transport measurements on homogeneous films strongly suggest that the transition out of the superconducting state in these films involves the collapse of the amplitude of the superconducting order parameter and a concomitant rise in the quasi-particle density. Experiments have shown that on approaching the transition region from the superconducting side, the mean field transition temperature decreases and simultaneously, the size of the energy gap decreases [14]. In fact, very close to the transition, the energy gap appears to go to zero [4]. Since the energy gap gives a direct measure of the order parameter amplitude, these earlier tunneling measurements intimate that the amplitude of the superconducting order parameter goes to zero as superconductivity disappears.

In addition, as  $\Delta$  decreases, the tunneling density of states assumes an increasingly broadened BCS form [15] as shown by Fig. 2. The differential tunnel junction conductances for these two PbBi/Ge films were obtained at a reduced temperature of  $t \simeq 0.2$  and normalised by the voltage-dependent normal state conductance (see Ref. [15] for

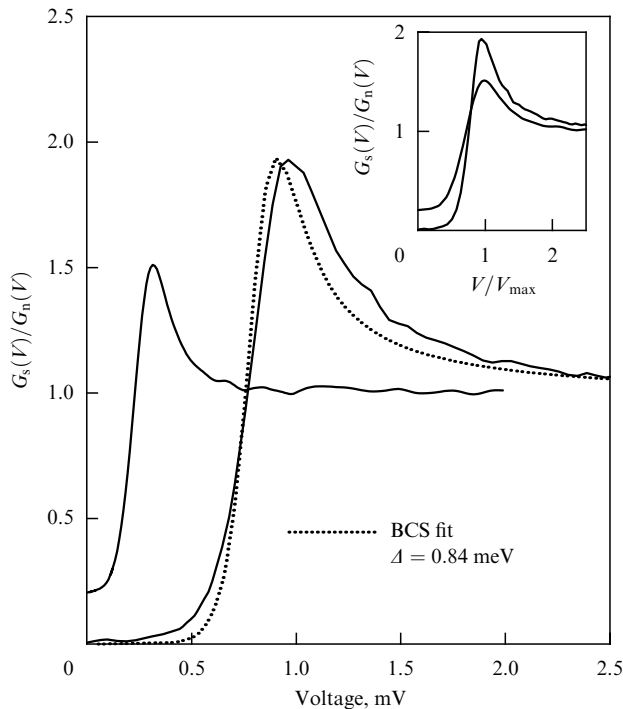


**Figure 2.** Normalized tunnel-junction conductance of superconductor (PbBi/Ge)–insulator–normal metal tunnel junctions for two different PbBi/Ge films ( $T_{c0} = 4.43$  and  $1.64$  K). The data (solid lines) were taken at a reduced temperature of  $\approx 0.2$  and have been normalized by the conductance of the junction in a magnetic field high enough to suppress superconductivity. The higher  $T_{c0}$  film is fit well using the BCS form for the density of states (dotted line). The inset shows the same data with the voltage axis scaled by the peak position in each data set. If both conductances followed BCS predictions, their peaks and low bias conductances would be equal and a simple rescaling of the voltage axis would collapse the two curves together.

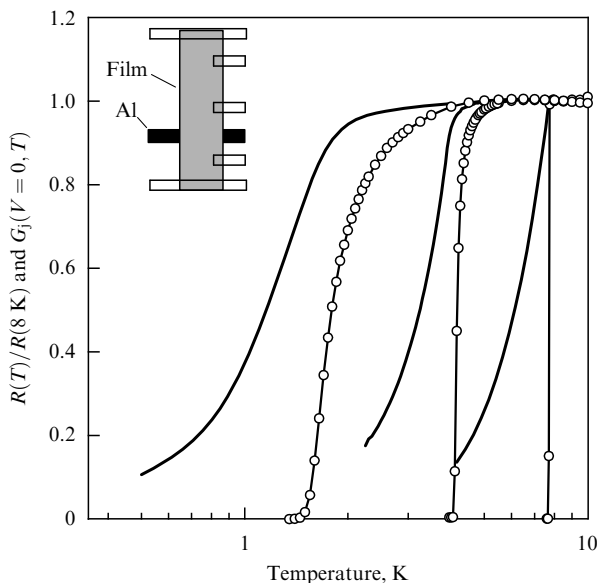


**Figure 3.** Sheet resistance (lines with open circles) and tunnel junction zero-voltage-bias conductance (ZBC) (solid lines) as a function of temperature for three PbBi/Ge films. To facilitate comparison, the sheet resistances have been normalized to their value at 8 K and the ZBC have been normalized to their value at the highest temperature at which data is shown.

procedure). The voltage dependence in the normal state results from disorder enhanced Coulomb interaction effects and is well understood [16]. Qualitatively, the tunnel junction conductances of both films exhibit the expected BCS form including a peak and a gap. Quantitatively, the film with the larger gap fits the BCS form well. However, the conductance of the junction on the film with the smaller energy gap, which is closer to the transition region, is higher in the gap region and the peak is substantially lower than expected for a BCS superconductor. The inset of Fig. 2, in which the same data are plotted on a voltage scale normalised to the peak in the conductance, emphasizes these deviations. For BCS superconductors with different gaps, conductances measured at the same reduced temperature should fall upon one another when the voltage axis is scaled in this fashion. Clearly, the peak is smaller and relatively broader and the conductance in the ‘gap’ is substantially higher than BCS theory predicts. These qualitative deviations from BCS behavior continue to grow upon approaching the transition region [17].

Fluctuation effects are also apparent in the tunneling and transport in homogeneous films at temperatures in the vicinity of  $T_{c0}$  [19]. Figure 3 shows the zero voltage bias conductance (ZBC) of a tunnel junction on and the resistance of thin homogeneous PbBi/Ge films as a function of temperature. To facilitate comparison of the tunneling and transport data among different films, the ZBC’s are normalised to their values at 8 K and the resistances are normalised to their maximum value. The ZBC is proportional to the number of quasi-particle states within  $4.8k_B T$  of the Fermi energy. In bulk conventional superconductors, the slope of the ZBC as a function of temperature changes discontinuously at  $T_{c0}$  where  $\Delta$  appears and the ZBC decreases rapidly with decreasing temperature. The film with the highest  $T_{c0}$  in Fig. 3 exhibits this behavior. Also, the resistive transition for this film is sharp and occurs with the kink in the ZBC. As  $T_{c0}$  decreases, the kink in the ZBC rounds and its drop becomes more gradual. Concomitantly, the resistive transition, which occurs near the same temperature as the gap opening, becomes broader. While some broadening near  $T_{c0}$  and above is expected, the broadening near the transition region is greater than conventional expectations (see below). It is important to note that for each of the three films, the opening of the energy gap and the resistive transition midpoint, i.e.  $T_{c0}$ , roughly coincide. This coincidence implies that the quasiparticle density is high at and above  $T_{c0}$ . Correspondingly, the order parameter amplitude is very small and susceptible to thermal fluctuations in the region where the broadening of the resistive transitions occurs. In other words, this broadening of the resistive transitions corresponds to a growth of the paraconductance or amplitude fluctuation dominated portion of the superconducting transition.

Analysis of the transport data shown in Fig. 1 suggests that the size of the paraconductance fluctuation dominated regime diverges as  $T_{c0}$  decreases [18]. To accurately measure the size of this regime it is necessary to know the temperature dependence of the normal state conductance. For ‘clean’ materials this dependence is very weak and often negligible. In these strongly disordered films the temperature dependence is too strong to ignore, but well understood. It stems from weak localization and electron–electron interaction effects and these effects lead to a temperature dependence of the conductance that varies little with film sheet resistance. Figure 4 demonstrates this weak dependence, showing the conductances of a few Bi/Sb films near the transition

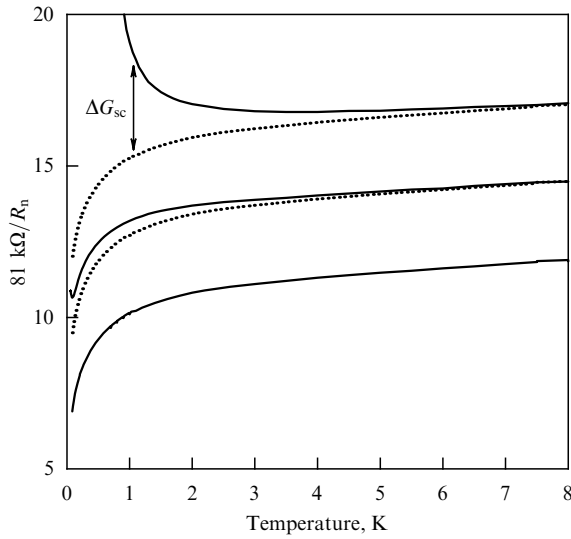


**Figure 4.** Sheet conductance as a function of temperature for the three BiSb films closest to the superconducting-to-nonsuperconducting transition in Fig. 1 (solid lines). The dotted lines are the conductance of the lowest conductance curve shifted to coincide at high temperatures with the conductances of the two higher conductance curves, which exhibit superconducting fluctuations. We presume that the dotted curves provide an accurate description of the normal-state conductances of each of the films and use it to calculate the superconducting fluctuation contribution  $\Delta G_{sc}$  to the temperature dependence of the conductance.

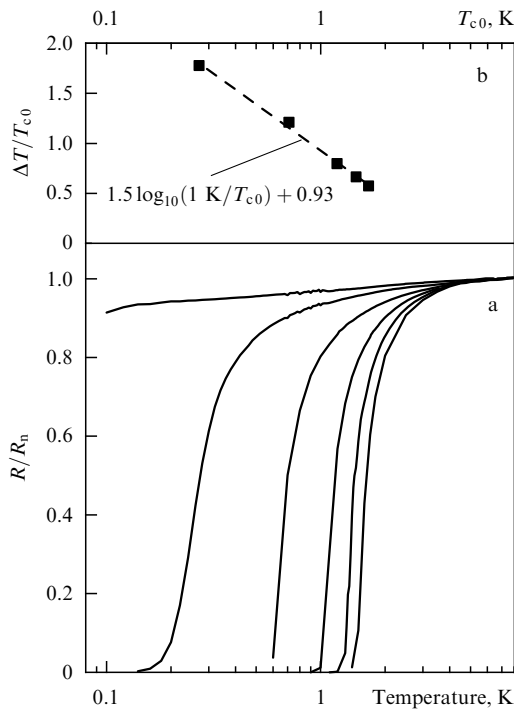


**Figure 5.** (a) Normalized sheet resistance of Bi/Sb films near the superconducting-to-nonsuperconducting transition as a function of temperature. The normalized resistance is obtained from  $R/R_n = 1 - R\Delta G_{sc}$ , where  $R(T)$  is the sheet resistance and  $\Delta G_{sc}$  is obtained as described in Fig. 4. Note the increasing breadth of the transitions as  $T_{c0}$  decreases. (b) Normalized transition width plotted versus the temperature of the midpoint of the transition on a logarithmic scale. The width is defined by  $\Delta T = T(R/R_n = 0.9) - T(R/R_n = 0.1)$ . The dashed line is a least-square fit to the data.

between the superconducting and nonsuperconducting states. The lowest conductance film exhibits no signs of superconductivity while the two upper films both show a conductance that increases with decreasing temperature at the lowest temperatures. We use the temperature dependence of the conductance of the lowest conductance film shown to determine the size of the paraconductance fluctuations,  $\Delta G_{sc}$ , as shown in Fig. 4. Normalised resistive transitions, obtained using  $\Delta G_{sc}$  (see Fig. 4 caption), are shown in Fig. 5a for films near the transition. Clearly, the relative breadth of the superconducting transitions grows as  $T_{c0}$  decreases. In the case of the film closest to the transition, whose resistance drops by less than 10% down to 0.1 K, superconducting fluctuation effects are apparent over a factor of more than 30 in temperature! More quantitatively, the widths corresponding to the temperature interval over which the resistance drops from 90% to 10% of its normal-state value, normalised by  $T_{c0}$  are plotted in Fig. 5b.  $T_{c0}$  is estimated by the temperature at which the film sheet resistance has fallen to half its normal-state value. As shown, the width appears to diverge logarithmically as  $T_{c0}$  goes to zero.

#### 4. Discussion

The characteristics of the deviations of the tunneling conductances and resistively measured transitions from the simple mean-field BCS form provide strong evidence that fluctuations in the amplitude of the superconducting order parameter grow upon approaching the SNST in homogeneous films. Near the transition, the tunneling data cannot be fit to the simple BCS form using a single energy gap: the peaks are too broad and the ZBC is too large indicating states at and near the Fermi energy in the superconducting state. Taken together, these imply that the amplitude of the order parameter, which is proportional to  $\Delta$ , is not well defined and may be zero in certain regions of a film. The growth and apparent divergence of the width of the resistive transitions over the temperature interval where tunneling indicates that the energy gap has barely opened and hence, the order parameter amplitude is small, intimates that fluctuations in the amplitude of the superconducting order parameter become critical at the SNST.

At the high sheet resistances considered here,  $R_n \simeq R_Q$ , there are a few factors that could contribute to the increasing breadth of the density of states, the broadening of the ZBC temperature dependence, and the broadening of the resistive transitions. First, inelastic quasi-particle scattering processes become stronger with increasing sheet resistance and these processes reduce the quasi-particle lifetime [6]. The reduced lifetimes broaden the structure in the quasi-particle density of states and thus, the tunnel junction conductance. They also increase the density of low energy excitations which increases the ZBC and broaden its temperature dependence. While such inelastic scattering effects are in the nonperturbative regime at these sheet resistances, they should still disappear at low temperatures. Thus, they probably cannot explain all of the broadening indicated in Fig. 3 because those data were taken at a relatively low reduced temperature of 0.2.

There are two other factors that could be responsible for the low-temperature broadening. Mesoscopic fluctuations in the density of electronic states near the Fermi energy could give rise to fluctuations in the amplitude of the pairing potential and the energy gap that would persist in the low temperature limit [5]. For  $R_n \simeq R_Q$  these fluctuations are

expected to be of order unity. Also, the SNST could be a quantum phase transition with associated critical point amplitude fluctuation effects. Recent theories (see, for example [7, 8]) predict the growth of fluctuations in the superconducting order parameter amplitude that diverge at the transition. The conductance of a large area tunnel junction measures a density of states averaged over these fluctuations. It should be broader than the density of states for a BCS superconductor with a single gap. The resistively measured transition would be sensitive to the accompanying spatial distribution of  $T_{c0}$ 's in the film and would also become broader. In two dimensions, the predicted divergence for a superconductor-to-normal metal transition is logarithmic [8], in accord with the result shown in Fig. 5b.

The above results and discussion suggest a qualitatively different picture of the SNST for homogeneous films than the 'standard' dirty boson models of the SIT (see, for example [9]). In the latter, increasing the normal state sheet resistance decreases the Josephson coupling between individually superconducting islands in the film. The concomitant reduction in the superfluid density or phase modulus leads to the growth of phase fluctuations between the islands. If the phase fluctuations are large enough, all phase coherence is lost, Cooper pairs become localized to their individual islands, and the system becomes an insulator [9, 10]. In contrast, in the homogeneous films considered here, the growing amplitude fluctuations increase the quasi-particle density. This increase comes at the expense of the Cooper pair or superfluid density. At high enough sheet resistances the superfluid density is driven to zero and a nonsuperconducting phase consisting of weakly localized quasi-particles takes over.

## 5. Conclusions

We have presented electron tunneling and transport measurements on homogeneous films that provide evidence that fluctuations in the superconducting order parameter amplitude grow as the amplitude collapses at the SNST. These fluctuation effects dominate the experimentally accessible portion of the resistive transitions of the films closest to the SNST. Theories suggest that the mesoscopic fluctuation, quasi-particle lifetime, and quantum critical fluctuation effects could each contribute to the growth of the amplitude fluctuations. Taken as a whole, our results suggest that amplitude fluctuations become so strong near  $R_n \simeq R_Q$  that they drive the superfluid density to zero to destroy the superconducting state.

We wish to acknowledge the support of NSF grants DMR-9801983 and DMR-9502920 and helpful conversations with Fei Zhou, Brad Marston, Boris Spivak, Nandini Trivedi, Sean Ling, and Dietrich Belitz.

## References

1. See, for example, Finkel'stein A M *Physica B* **197** 636 (1994) and references therein
2. Belitz D, Kirkpatrick T R *Rev. Mod. Phys.* **66** 261 (1994)
3. Haviland D B, Liu Y, Goldman A M *Phys. Rev. Lett.* **62** 2180 (1989)
4. Valles J M, Jr, Dynes R C, Garno J P *Phys. Rev. Lett.* **69** 2180 (1992)
5. Spivak B, Zhou F *Phys. Rev. Lett.* **74** 2800 (1995)
6. Devereaux T P, Belitz D *Phys. Rev. B* **43** 3736 (1991)
7. Ghosal A, Randeria M, Trivedi N *Phys. Rev. Lett.* **81** 3940 (1998)
8. Kirkpatrick T R, Belitz D *Phys. Rev. Lett.* **79** 3042 (1997)
9. Fisher M P A, Grinstein G, Girvin S M *Phys. Rev. Lett.* **64** 587 (1990)

10. Hebard A F, in *Strongly Correlated Electronic Materials* (Ed. K Bedell) (Reading, Mass.: Addison-Wesley, 1993); Goldman A M, Markovic N *Phys. Today* **51** (11) 39 (1998)
11. Hsu S-Y, Ph D Thesis (Brown University, 1995)
12. Strongin M et al. *Phys. Rev. B* **1** 1078 (1970)
13. Ekinici K L, Valles J M, Jr *Phys. Rev. B* **58** 7347 (1998)
14. Dynes R C et al. *Phys. Rev. Lett.* **57** 2195 (1986)
15. Hsu S-Y, Chervenak J A, Valles J M, Jr *Phys. Rev. Lett.* **75** 132 (1995)
16. Hsu S-Y, Valles J M, Jr *Phys. Rev. B* **49** 16600 (1994)
17. Valles J M, Jr et al. (in preparation)
18. Chervenak J A, Valles J M, Jr *Phys. Rev. B* **59** 11209 (1999)
19. Hsu S-Y, Chervenak J A, Valles J M, Jr *J. Phys. Chem. Solids* **59** 2065 (1998)

## Vortex states at low temperature in disordered thin and thick films of a-Mo<sub>x</sub>Si<sub>1-x</sub>

S Okuma, M Morita

**Abstract.** We have measured the ac complex resistivity in the linear regime, as well as dc resistivity, for thick (100, 300 nm) amorphous (a-)Mo<sub>x</sub>Si<sub>1-x</sub> films at low temperatures ( $T > 0.04$  K) in constant fields  $B$ . The critical behavior associated with the second-order transition has been observed for both dc and ac resistivities, which is similar to that observed for granular indium films. This is the first convincing evidence for the vortex glass transition (VGT) in the homogeneously disordered low- $T_C$  superconductors containing microscopic pinning centers. We have found that the VGT persists down to  $T \sim 0.1 T_{C0}$  up to  $B \sim 0.9 B_{C2}(0)$ , where  $T_{C0}$  and  $B_{C2}(0)$  are the mean-field transition temperature and upper critical field at  $T = 0$ , respectively. At  $T \rightarrow 0$  the VGT line  $B_g(T)$  extrapolates to a field below  $B_{C2}(0)$ , indicative of the presence of a  $T = 0$  quantum-vortex-liquid phase in the region  $B_g(0) < B < B_{C2}(0)$ .

For thin (4 nm) films the ( $T = 0$ ) field-driven superconductor-insulator transition takes place at  $B_C$ . We have not obtained evidence of the metallic quantum liquid phase below  $B_C$ , while in  $B > B_C$  an anomalous negative magnetoresistance (MR) suggesting the presence of the localized Cooper pairs has been observed. The negative MR is commonly observed for thin films; however, for thick films the MR is always positive. This means that the two-dimensionality plays an important role in the appearance of the negative MR (or localized Cooper pairs). The negative MR is no longer visible as the field is applied parallel to the film surface, consistent with the view that mobile vortices, as well as localized Cooper pairs, are present in  $B > B_C$ .

## 1. Introduction

The superconductor-insulator transition (SIT) in two dimensions (2D) has been thoroughly studied during recent years [1–16]. While most of the studies have focused on the electronic states near the SIT, the vortex states at low temperature have not yet been well clarified. In moderately

S Okuma, M Morita Research Center for Very Low Temperature System, Tokyo Institute of Technology, 2-12-1, Ohokayama, Meguro-ku, Tokyo 152-8551, Japan